ELSEVIER

Contents lists available at ScienceDirect

Algal Research

journal homepage: www.elsevier.com/locate/algal





The effects of CdSe/ZnS quantum dots on the photosynthesis rate of the *Chlorella Vulgaris* beads

Wimeth Dissanayake ^{a,b}, Richard Hailstone ^c, Leslie Castillo ^d, Fateme "Sara" Nafar ^e, Mengdi Bao ^e, Ruo-Qian Wang ^f, Colin Gates ^d, Xin Yong ^g, Ke Du ^{a,e,*}

- ^a Department of Mechanical Engineering, Rochester Institute of Technology, Rochester, NY 14623, USA
- ^b Pittsford Mendon High School, Pittsford, NY 14534, USA
- ^c NanoImaging Lab, Chester F. Carlson Center for Imaging Science, Rochester Institute of Technology, Rochester, NY 14623, USA
- ^d Department of Chemistry and Biochemistry, Loyola University Chicago, Chicago, IL 60660, USA
- e Department of Chemical and Environmental Engineering, University of California, Riverside, CA 92521, USA
- f Department of Civil and Environmental Engineering, Rutgers, The State University of New Jersey, NJ 08854, USA
- g Department of Mechanical Engineering, Binghamton University, The State University of New York, Binghamton, NY 13902, USA

ARTICLE INFO

Keywords: Microalgae Beads Quantum dots Photosynthesis Fluorescence Exocytosis

ABSTRACT

Photosynthesizing microalgae produce >50 % of oxygen in the atmosphere and are crucial for the survival of many living systems such as coral reefs. To address the declining of coral reefs, artificial reefs have been introduced to encapsulate the microalgae cells in a polymer matrix but the effects of nanoscale pollutants on these engineered systems have not been fully understood. In this work, quantum dots with a size smaller than 10 nm are being used to elucidate the photosynthesis performance of the sodium alginate beads encapsulated with Chlorella vulgaris (C. vulgaris). The fluorescent quantum dots can move into the alginate matrix and the fluorescence intensity in the algae beads is correlated with the quantum dot concentration. We further show that the photosynthesis of the algae beads is sensitive to the quantum dot concentration and are also time sensitive. In the first 48 min of quantum dot exposure, both carbon dioxide absorption and oxygen production are low, suggesting limited photosynthesis. After the initial incubation, the photosynthesis rate quickly increases even though more inhibition is still observed with higher concentration of the quantum dots. The measured electron transport rate shows a similar trend and is also sensitive to the quantum dot concentration.

1. Introduction

Green algae, such as *Chlorella vulgaris* (*C. vulgaris*), are crucial to the marine systems via the formation of symbiotic relationships with other organisms, particularly coral reefs [1,2]. In recent years, engineering living systems containing algae cells have been introduced to mimic the morphological features of coral reefs, showing enhanced photosynthetic efficiency [3,4]. However, an emerging challenge for coral reefs and engineering living reefs is the continuous exposure to chemical waste, especially at nanoscale [5,6]. Early results reported decreases in cell growth rate and chlorophyll content when the cell cultures were exposed to nanomaterials such as quantum dots [7], nanoplastics [8], and oxide nanoparticles [9]. To date, most of the research on nanomaterials/microalgae interactions has focused on cell cultures in solution, and little has been investigated with the immobilized microalgae

cells that can be constructed as engineering living systems.

Here, we use streptavidin-coated quantum dots as a model to study the interaction of nanostructures with engineering living systems by encapsulating *C. vulgaris* in sodium alginate beads (Fig. 1a). We show that more quantum dots are presented in the algae beads as the quantum dot concentration in the solution increases. In the first 48 min after incubation, the photosynthesis is significantly inhibited by the presence of quantum dots. However, the photosynthesis rate increases after the initial incubation, suggesting that some of the quantum dots might be released or digested by the algae cells. At 120 min, algae beads incubated with quantum dots show less oxygen production than the samples without quantum dots, and the oxygen production is inversely correlated with the quantum dot concentration. In addition, we show that the effective photochemical yield in the microalgae is also sensitive to the quantum dot concentration and incubation time as the electron

^{*} Corresponding author at: Department of Chemical and Environmental Engineering, University of California, Riverside, CA 92521, USA. *E-mail address:* kdu@ucr.edu (K. Du).

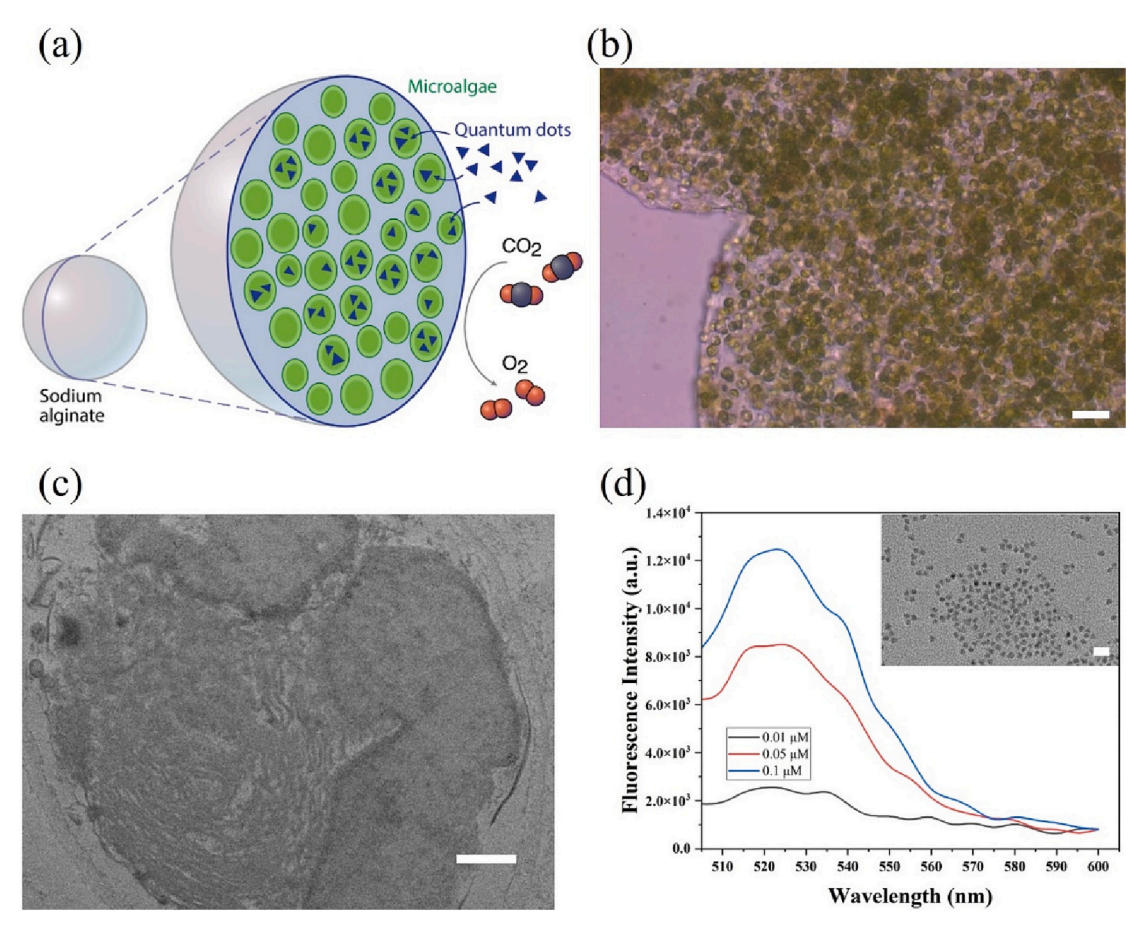


Fig. 1. (a) The schematic showing the endocytosis and photosynthesis process of microalgae beads with quantum dots. (b) Bright-field image of the algae beads (scale bar: 20 μm). (c) TEM image of a microalgae cell (scale bar: 400 nm). (d) Measured uncorrected emission curve versus streptavidin-coated quantum dots. Inset is the TEM image of the quantum dots (scale bar: 20 nm).

transport rate (ETR) drops with time but slightly recovers after 100 min. These results indicate that the microalgae-based living systems are sensitive to the environment with nanoscale pollutants.

2. Materials and methods

2.1. Materials

C. vulgaris beads were obtained from Algal Research Supply and were manufactured using Sodium Alginate and Calcium Chloride [10]. The bright field and TEM image of a dissected bead are shown in Fig. 1b and c, respectively. Algal cultures were purchased from Algal Research Supply and grown using Bold's Basal Medium. Streptavidin - ZnS/CdSe quantum dots (5 nm size), with 525 nm emission maxima, were purchased from Thermofisher Scientific. The uncorrected emission curve of quantum dots with a concentration ranging from 0.01 to 0.1 μM is shown in Fig. 1d. Philips T12, 40-watt, cool white fluorescent lights were used to incubate and grow the microalgae cells on a 12 h/12 h light-dark cycle.

2.2. Incubation of microalgae beads with quantum dots

Ten microalgae beads were placed into a 200 μL PCR tube with 100 μL of quantum dot solution (0 to 0.1 $\mu M).$ The solution was first mixed for 2 min, then centrifuged at 1500 rpm for 15 min, followed by 90 min of room temperature incubation under a T12, cool white, fluorescent light.

2.3. Production of CO₂

Stored CO₂ was generated by the chemical reaction:

$$CaCO_3 + 2HCl \ge CaCl_2 + CO_2 + H_2O$$
 (1)

Two 4-l sealable glass containers were connected by Teflon tubing. We added 22 mL of HCl to one of the containers and followed by another 47 g of CaCO $_3$. The glass was then promptly sealed, only allowing gas to pass through the Teflon tubing into the second container, separating CO $_2$ from other products. Using a thin 100 μ L Hamilton syringe, 3.6 L of CO $_2$ gas was extracted from the second container for later use.

2.4. Quantification of chlorophyll amount

One milliliter of Na-Citrate solution (0.1 M) was added to the beads solution and vortexed for 1 min. After 1 h of incubation at room temperature, the sample was washed with 1 mL of PBS solution for 1 min. The cell pellets were collected by centrifuge at 15,000 rpm for 5 min [11]. Then, the cells were added into 4 mL of 80 % acetone and heated in a water bath at 55 °C for 30 min in dark. After centrifuging at 12,000 rpm for 5 min, the supernatant was diluted to 5 mL and the absorbance at 646 and 663 nm were measured. Finally, the content of chlorophyll a, b, and total were calculated with the following formula [12,13]:

$$C_a = 12.21A_{663} - 2.81A_{646} \tag{2}$$

$$C_b = 20.13A_{646} - 5.03A_{646} \tag{3}$$

$$C_T = C_a + C_b \tag{4}$$

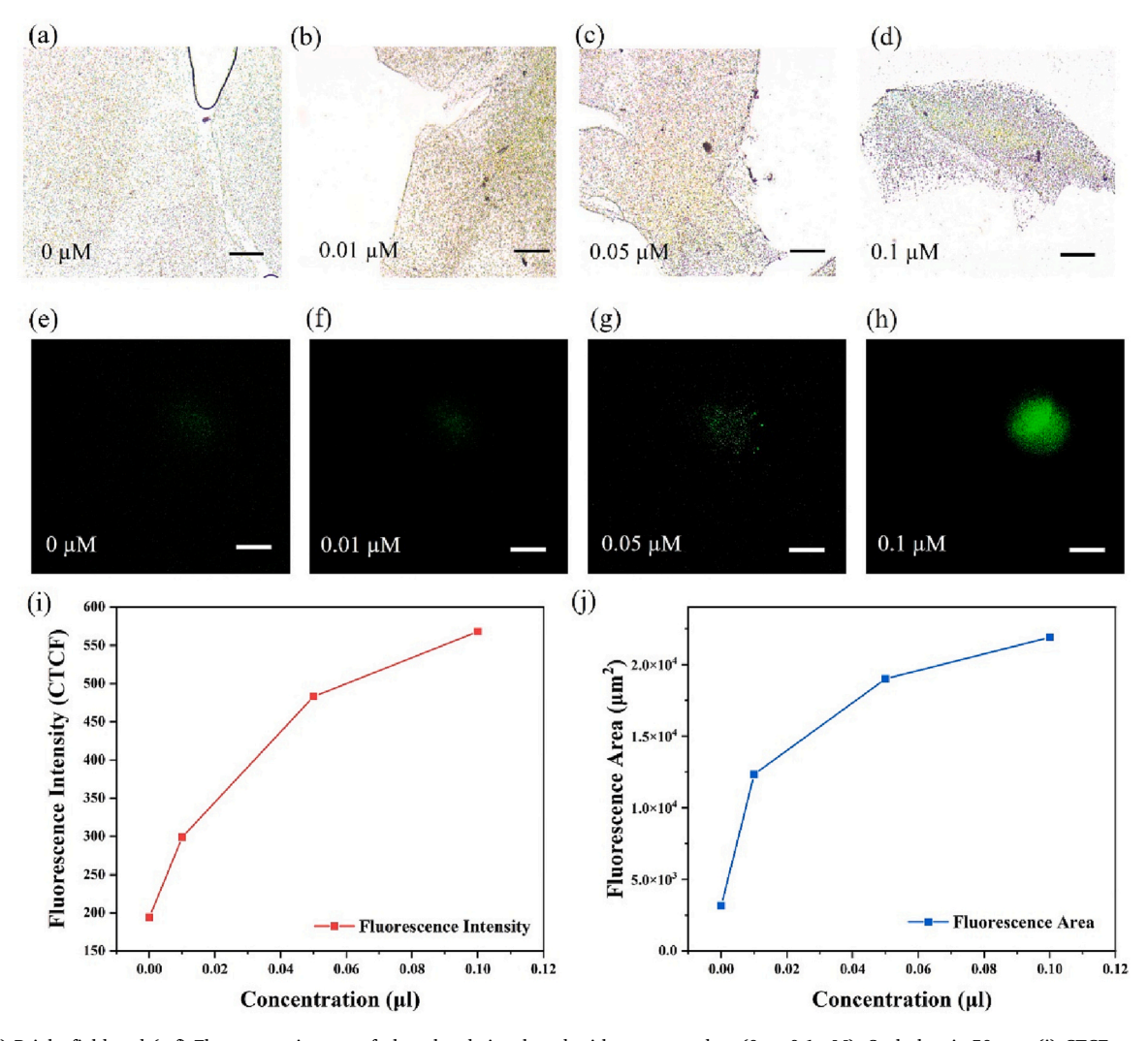


Fig. 2. (a-d) Bright-field and (e-f) Fluorescent images of algae beads incubated with quantum dots (0 to 0.1 μ M). Scale bar is 50 μ m. (i) CTCF graphed and (j) Fluorescence area of algae beads versus quantum dots ranging from 0 to 0.1 μ M.

where C_a , C_b , C_T are chlorophyll a, b and total chlorophyll respectively.

2.5. Measurement of ETR

ETR under the same incubation conditions was measured according to the method of Genty [14]. A customized JTS-150 spectrometer (SpectroLogiX, Knoxville, TN USA) was used to perform all fluorescence measurements. Ambient fluorescence under incubation light (ΔF) was obtained, after which culture was briefly (90 s) dark-adapted and Fo' and Fm' were obtained using a pulse-amplitude modulation type multiple-turnover pulse of light delivered for 50 ms from a 630 nm LED at 7,000 mmol photons m $^{-2}$ s $^{-1}$. C. vulgaris, as for most Chlorellas, has approximately 1:1 photosystem stoichiometry and thus ETR could be calculated as described in Kromkamp and Forster [15] considering the chlorophyll concentration obtained previously and an optical absorption area in sample cuvette of $25\times 10^{-6}~\text{m}^2$.

3. Results and discussions

An Amscope XD-RFL microscope with a 475AF40 exciter and a 535AF45 emitter was used to image the microalgae beads. A Dichroic of 505DRLP was used to block the excitation. Several areas of the cells containing quantum dots were analyzed against the areas without quantum dots. The baseline for fluorescence was calculated by the

following equation:

The area of fluorescence was identified by using threshold values of 83 and 87 HSG, the values most closely matched the emission of the quantum dots, to isolate the fluorescence of the quantum dots. After isolation, the area of these regions was integrated to obtain a total area of fluorescence. We found that increasing the quantum dot concentration from 0 to 0.1 μ M increases the CTCF value of the microalgae beads (Fig. 2a-h). The calculated CTCF value and the total fluorescence area shown in Fig. 2i and j, respectively. They both present a logarithmic relationship with the quantum dot concentration, indicating that the uptake capacity for the cells decreases with the increasing amount of the quantum dots. Even though it is challenging to directly quantify the number of quantum dots absorbed into the beads, we compared the fluorescence signal of the remaining quantum dots (input concentration of 0.1 μ M) in the supernatant of the beads solution and found that most of the quantum dots were absorbed within 20 min (Supplement Fig. 1).

Next, we investigated the changes in the rate of photosynthesis at different concentrations of the quantum dots through a bicarbonate indicator solution, which comprises a pH indicator and HCO_3^- ions. At higher levels of CO_2 , the number of HCO_3^- increases, resulting in a decrease in pH and a corresponding color change from orange to yellow

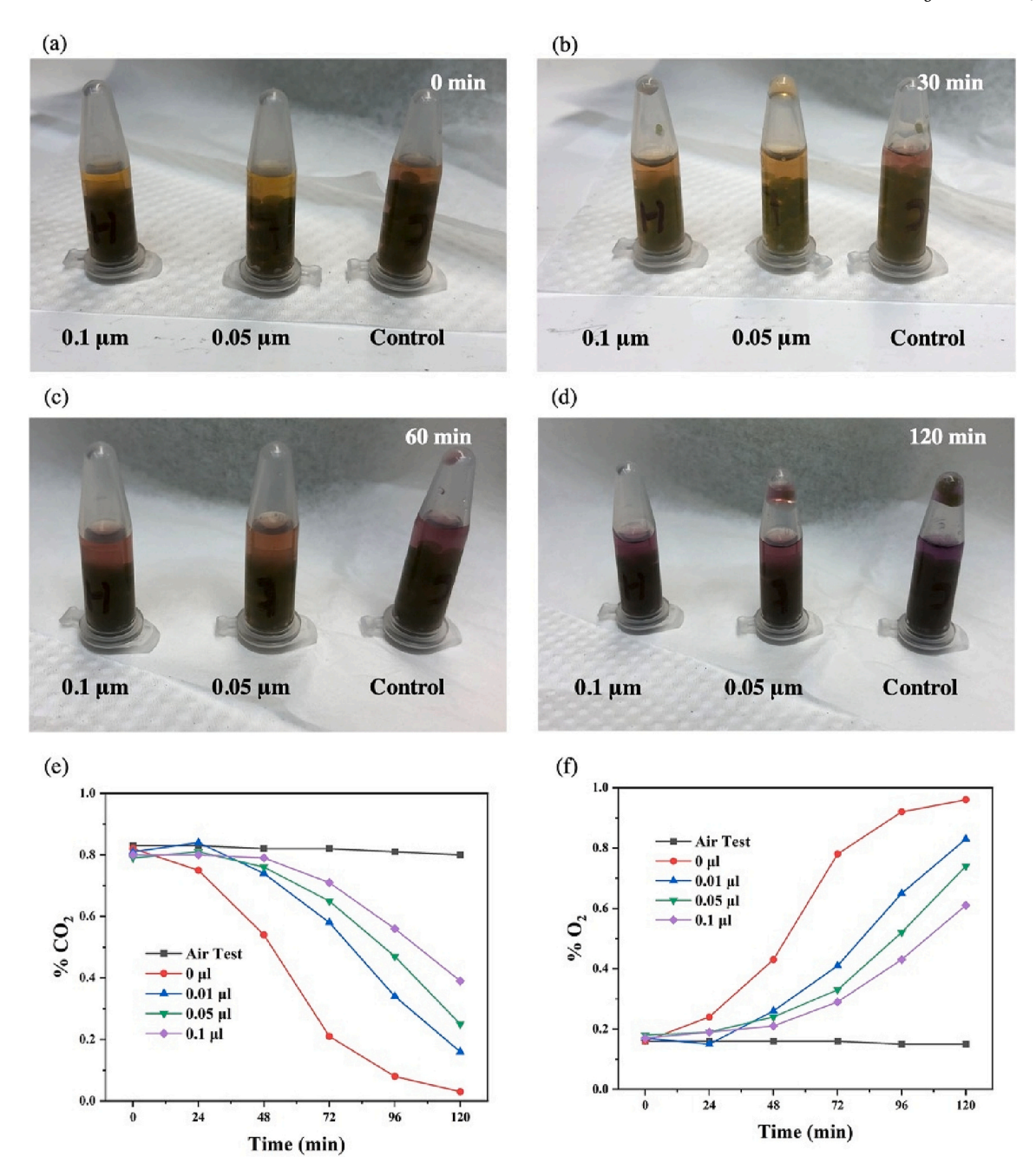


Fig. 3. Qualitative analysis of the photosynthesis rate using bicarbonate indicator for quantum dots ranging from 0 to 0.1 μ M and an incubation time of (a) 0 min. (b) 30 min. (c) 60 min. (d) 120 min. (e) CO₂ and (f) O₂ level versus time of the alginate beads solution with different concentrations of the quantum dots.

hue. In contrast, lower levels of CO_2 reduce the number of HCO_3^- and thus increase pH, causing the solution color changing to a purple or blue hue. The characterization starts with the preparation of $100~\mu L$ of bicarbonate indicator and $25~\mu L$ of CO_2 , and then incubated for 30~s, allowing the red-hued indicator to turn yellow. Afterward, five beads were added to the solution, which were subsequently sealed and illuminated with white fluorescent light for 2~h. Every 30~min, the solution was mixed at low speed for 30~s and then photographed. As shown in Fig. 3a-d, the rate of pH change in the solution is lowered with increasing quantum dot concentration, confirming a negative correlation between quantum dot concentration and the rate of algae photosynthesis.

Following that, gas chromatography—mass spectrometry was used to quantify the concentration of CO_2 and O_2 in the microalgae beads solution. Five beads with different concentrations of the quantum dots (0

to 0.1 uM) were added to the chromatography vials. The 200 μL of CO2 were added at time 0, after which the solutions were placed under a fluorescent lamp. At 24 min, 200 μL of CO2 were added to the second set of the solutions, which were placed under a fluorescent lamp. This process was repeated for all sets of solutions until the last set produced at 120 min. As shown in Fig. 3e, the CO2 concentration present in the beads over time is positively correlated with the concentration of quantum dots. The O2 concentration in the beads over time is negatively correlated with the concentration of quantum dots (Fig. 3f). These quantitative data confirm a decrease in the rate of photosynthesis as the concentration of quantum dots increases.

As shown in Fig. 4, in the absence of quantum dots, ETR in beads exposed to incubation conditions initially remains constant but declines after approximately an hour. Addition of increasing concentrations of quantum dots causes a more rapid decline in electron transport rate,

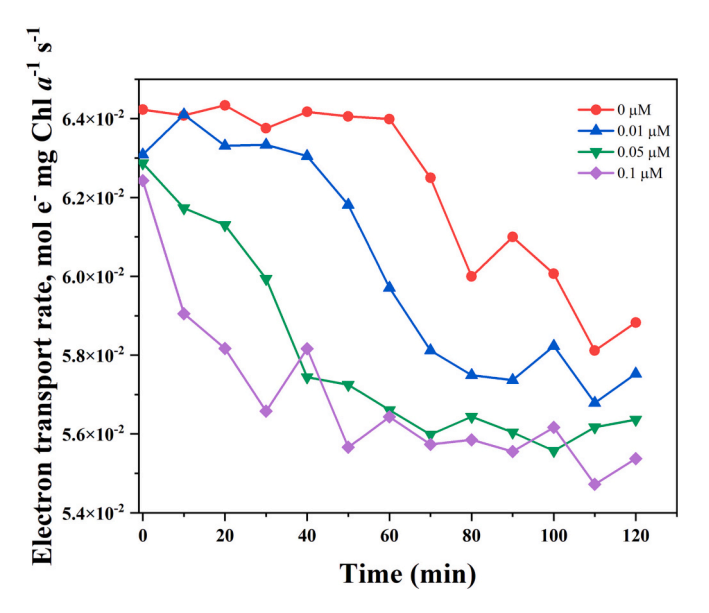


Fig. 4. Electron transport rate in illuminated algae beads incubated with quantum dots at concentrations ranging from 0 to 0.1 μ M. ETR was measured every 10 min.

with an immediate decline observed at a concentration of 0.1 µM. The electron transport rates observed are very low as compared to liquid cultures of green algae, which would be expected to generate several times more electrons per chlorophyll assuming a conventional antenna size, but this can be explained by the difference between a highly scattering liquid culture and shading algal beads. This shading both impedes delivery of stimulating light to culture and impedes fluorescence observation of cells not near the surface of the bead facing the light source as a considerable concentration of algae will be found in fixed positions near enough that shading is a concern. Nevertheless, what algae are observed to be photosynthetically active are affected by quantum dot concentration. The midpoint of the fluorescence decay kinetic shifts from some time after 1 h (unclear, as the culture never reached a stable post-inactivation fluorescence level) in beads incubated without quantum dots to about 1 h at 0.01 μ M, 30–35 min at 0.05 μ M, and finally a mere 10–15 min at 0.1 μM . The cells negatively impacted by quantum dots appear to be so affected in a concentration-dependent and thus likely diffusion-limited manner. Considering that the ETR reaches a relatively stable minimum with $>\!85$ % of initial electron transport still occurring in the presence of any tested concentration of these quantum dots, long-term inhibition of photosynthesis is clearly limited.

The scale-up of microalgae cultivation with photosynthesis requires living systems based on microalgae cells and polymer matrix to be created with high spatial cell densities [3]. However, the influence of engineering nanomaterials and debris on these living systems has not been explored [9,16]. Despite that alginate and other polymer building blocks can immobilize the cells and impede the quantum dots uptake [17], we have found that the photosynthesis of the algae beads remains significantly affected, especially within the first 48 min after the incubation. Previous studies have found a correlation between the introduction of nanostructures to aquaponics plants and the inhibition of the cell wall functions [18,19]. The quantum dots could have similar adverse effects by inhibiting the vital movement of resources needed for photosynthetic activity in the algae beads, thus indirectly causing the plants' rate of photosynthesis to decrease. Another possible cause is that the quantum dots directly interfere with the cells' light absorption in the matrix [20]. This mechanism would decrease photosynthesis, but not cellular respiration, unlike the inhibition of the cell walls.

We found that the photosynthetic rate increases over time for the

algae beads incubated with the quantum dots, regardless of the quantum dot concentration. For example, at 72 min, the O2 level is only 0.3 % for the $0.1~\mu L$ sample, compared to 0.8~% without quantum dots. On the other hand, at 120 min, the difference between the two samples decreases to ~ 0.3 %. As the pore size on the cell wall is 5-20 nm, the quantum dots can enter the cell wall through endocytosis to damage the cell structure, thus lowering the photosynthetic efficiency. However, the ubiquitous rate increase for all the samples indicates that the cells can adapt to the hazardous environment and still perform photosynthesis by exocytosis. Exocytosis is an important process for plant and animal cells to remove waste and rebuild cell membrane [21]. It is possible that the exocytosis of quantum dots increases after the initial 48 min of incubation, which explains the increase of O2 production and the recovery of ETR. In addition, other research has found that nanoparticles may store mostly in vacuole than entering cytoplasm, which allows the cells to resolve the nanotoxicity over time [22,23].

CRediT authorship contribution statement

Wimeth Dissanayake: Conceptualization, Methodology, Validation, Formal analysis, Investigation, Data Curation, Writing - Original Draft; Richard Hailstone: Methodology, Investigation, Data Curation; Leslie Castillo: Investigation, data curation; Fateme "Sara" Nafar: Investigation, data curation, writing; Mengdi Bao: Investigation, Data Curation, Writing - Review & Editing; Ruo-Qian Wang: Conceptualization, Writing - Review & Editing; Colin Gates: Investigation, data curation, writing, supervision; Xin Yong: Conceptualization, Methodology, Writing - Review & Editing, Supervision; Ke Du: Conceptualization, Methodology, Writing - Review & Editing, Supervision, Project administration, Funding acquisition.

Declaration of competing interest

Ke Du and Xin Yong report financial support was provided by National Science Foundation.

Data availability

Data will be made available on request.

Acknowledgements

This material is based upon work supported by the National Science Foundation under Grant 2034855 to Xin Yong and 2306229 to Ke Du. The authors would like to thank Xian Boles for the schematic design.

Appendix A. Supplementary data

Supplementary data to this article can be found online at https://doi.org/10.1016/j.algal.2023.103095.

References

- [1] J. Brodie, C.X. Chan, O. De Clerck, J.M. Cock, S.M. Coelho, C. Gachon, A. R. Grossman, T. Mock, J.A. Raven, A.G. Smith, H.S. Yoon, D. Bhattacharya, The algal revolution, Trends Plant Sci. 22 (8) (2017) 726–738, https://doi.org/ 10.1016/j.tplants.2017.05.005.
- [2] H. Teagle, S.J. Hawkins, P.J. Moore, D.A. Smale, The role of kelp species as biogenic habitat formers in coastal marine ecosystems, J. Exp. Mar. Biol. Ecol. 492 (2017) 81–98, https://doi.org/10.1016/j.jembe.2017.01.017.
- [3] D. Wangpraseurt, S. You, F. Azam, G. Jacucci, O. Gaidarenko, M. Hildebrand, M. Kühl, A.G. Smith, M.P. Davey, A. Smith, D.D. Deheyn, S. Chen, S. Vignolini, Bionic 3D printed corals, Nat. Commun. 11 (1) (2020) 1748, https://doi.org/ 10.1038/s41467-020-15486-4.
- [4] E. Riera, D. Lamy, C. Goulard, P. Francour, C. Hubas, Biofilm monitoring as a tool to assess the efficiency of artificial reefs as substrates: toward 3D printed reefs, Ecol. Eng. 120 (2018) 230–237, https://doi.org/10.1016/j.ecoleng.2018.06.005.
- [5] L.F.B. Marangoni, E. Beraud, C. Ferrier-Pagès, Polystyrene nanoplastics impair the photosynthetic capacities of symbiodiniaceae and promote coral bleaching, Sci.

- Total Environ. 815 (2022), 152136, https://doi.org/10.1016/j.
- [6] C. Ripken, K. Khalturin, E. Shoguchi, Response of coral reef dinoflagellates to nanoplastics under experimental conditions suggests downregulation of cellular metabolism, Microorganisms 8 (11) (2020) 1759, https://doi.org/10.3390/ microorganisms8111759.
- [7] S. Lin, P. Bhattacharya, N.C. Rajapakse, D.E. Brune, P.C. Ke, Effects of quantum dots adsorption on algal photosynthesis, J. Phys. Chem. C 113 (25) (2009) 10962–10966, https://doi.org/10.1021/jp904343s.
- [8] W. Yang, P. Gao, H. Li, J. Huang, Y. Zhang, H. Ding, W. Zhang, Mechanism of the inhibition and detoxification effects of the interaction between nanoplastics and microalgae chlorella pyrenoidosa, Sci. Total Environ. 783 (2021), 146919, https:// doi.org/10.1016/j.scitotenv.2021.146919.
- [9] M. Khoshnamvand, P. Hanachi, S. Ashtiani, T.R. Walker, Toxic effects of polystyrene nanoplastics on microalgae Chlorella vulgaris: changes in biomass, photosynthetic pigments and morphology, Chemosphere 280 (2021), 130725, https://doi.org/10.1016/j.chemosphere.2021.130725.
- [10] Ward's World Activity Guides How to Make Your Own Algae Beads. https://wardsworld.wardsci.com/i/1144195-how-to-make-your-own-algae-beads/0? (accessed 2022-05-31)
- [11] O. Murujew, R. Whitton, M. Kube, L. Fan, F. Roddick, B. Jefferson, M. Pidou, Recovery and reuse of alginate in an immobilized algae reactor, Environ. Technol. 42 (10) (2021) 1521–1530, https://doi.org/10.1080/09593330.2019.1673827.
- [12] Z. Yan, L. Xu, W. Zhang, G. Yang, Z. Zhao, Y. Wang, X. Li, Comparative toxic effects of microplastics and nanoplastics on chlamydomonas reinhardtii: growth inhibition, oxidative stress, and cell morphology, J. Water Process Eng. 43 (2021), 102291, https://doi.org/10.1016/j.jwpe.2021.102291.
- [13] Z. Zhao, L. Xu, Y. Wang, B. Li, W. Zhang, X. Li, Toxicity mechanism of silver nanoparticles to chlamydomonas reinhardtii: photosynthesis, oxidative stress, membrane permeability, and ultrastructure analysis, Environ. Sci. Pollut. Res. 28 (12) (2021) 15032–15042, https://doi.org/10.1007/s11356-020-11714-y.
- [14] B. Genty, J.-M. Briantais, N.R. Baker, The relationship between the quantum yield of photosynthetic electron transport and quenching of chlorophyll fluorescence,

- Biochim. Biophys. Acta Gen. Subj. 990 (1) (1989) 87–92, https://doi.org/10.1016/ S0304-4165(89)80016-9.
- [15] J.C. Kromkamp, R.M. Forster, The use of variable fluorescence measurements in aquatic ecosystems: differences between multiple and single turnover measuring protocols and suggested terminology, Eur. J. Phycol. 38 (2) (2003) 103–112, https://doi.org/10.1080/0967026031000094094.
- [16] S. Reichelt, E. Gorokhova, Micro- and nanoplastic exposure effects in microalgae: a meta-analysis of standard growth inhibition tests. Frontiers in environmental, Science (2020) 8.
- [17] X. Li, Z. Zhang, Q. Xie, D. Wu, Effect of algae on phosphorus immobilization by lanthanum-modified zeolite, Environ. Pollut. 276 (2021), 116713, https://doi.org/ 10.1016/j.envpol.2021.116713.
- [18] J. Ji, Z. Long, D. Lin, Toxicity of oxide nanoparticles to the green algae Chlorella sp, Chem. Eng. J. 170 (2) (2011) 525–530, https://doi.org/10.1016/j. cei 2010 11 026
- [19] A. Yan, Z. Chen, Impacts of silver nanoparticles on plants: a focus on the phytotoxicity and underlying mechanism, Int. J. Mol. Sci. 20 (5) (2019) 1003, https://doi.org/10.3390/ijms20051003.
- [20] G. Fan, Z. Chen, Z. Yan, B. Du, H. Pang, D. Tang, J. Luo, J. Lin, Efficient integration of plasmonic Ag/AgCl with perovskite-type LaFeO3: enhanced visible-light photocatalytic activity for removal of harmful algae, J. Hazard. Mater. 409 (2021), 125018, https://doi.org/10.1016/j.jhazmat.2020.125018.
- [21] G. Thiel, N. Battey, Exocytosis in plants, in: J. Soll (Ed.), Protein Trafficking in Plant Cells, Springer Netherlands, Dordrecht, 1998, pp. 111–125, https://doi.org/ 10.1007/978-94-011-5298-3.6
- [22] F. Chen, Z. Xiao, L. Yue, J. Wang, Y. Feng, X. Zhu, Z. Wang, B. Xing, Algae response to engineered nanoparticles: current understanding, mechanisms and implications, Environ. Sci.: Nano 6 (4) (2019) 1026–1042, https://doi.org/10.1039/ CRENO1368C
- [23] G. Pulido-Reyes, S.M. Briffa, J. Hurtado-Gallego, T. Yudina, F. Leganés, V. Puntes, E. Valsami-Jones, R. Rosal, F. Fernández-Piñas, Internalization and toxicological mechanisms of uncoated and PVP-coated cerium oxide nanoparticles in the freshwater alga chlamydomonas reinhardtii, Environ. Sci. Nano 6 (6) (2019) 1959–1972, https://doi.org/10.1039/C9EN00363K.